In search of effective H1N1 neuraminidase inhibitor by molecular docking, antiviral evaluation and membrane interaction studies using NMR

K. MALBARI[1], H. GONSALVES[1], A. CHINTAKRINDI[1], D. GOHIL[2], M. JOSHI[3], S. KOTHARI[2], S. SRIVASTAVA[3], A. CHOWDHARY[2], M. KANYALKAR[1*]

[1]Department of Pharmaceutical Chemistry, Prin K. M. Kundnani College of Pharmacy, Plot 23, Jote Joy Building, Rambhau Salgaonkar Marg, Cuffe Parade, Mumbai-400 005, India; [2]Haffkine Institute for Training, Research and Testing, Parel, Mumbai- 400 012, India; [3]National Facility for High Field NMR, Tata Institute of Fundamental Research, Homi Bhabha Road, Colaba, Mumbai-400 005, India

Summary. – Considering the need for discovery of new antiviral drugs, in view to combat the issue of resistance particularly to anti-influenza drugs, a series of 2'-amino, 3'-amino and 2', 4'-dihydroxy chalcone derivatives were designed. Structure-based drug design was used to design inhibitors of influenza virus – H1N1 neuraminidase enzyme. These were further optimized by a combination of iterative medicinal chemistry principles and molecular docking. Based on the best docking scores, some chalcone derivatives were synthesized and characterized by infrared spectroscopy (IR) and proton nuclear magnetic resonance (NMR). The molecules were evaluated for their anti-influenza action against influenza A/Pune isolate/2009 (H1N1) virus by *in vitro* enzyme-based assay (neuraminidase inhibition assay). We have then selected few of them for multinuclear NMR studies, ^{31}P NMR, in order to probe the molecular mechanism of their antiviral action. Reasonably good correlation between docking scores; anti-influenza activity; and ^{31}P NMR results were observed. The computational predictions were in consensus with the experimental results. It was observed that among tested compounds, derivative 1A, viz. 2', 4'-dihydroxy-4-methoxy chalcone, showed highest activity (IC_{50} = 2.23 μmol/l) against the virus under study. This derivative 1A can be explored further to provide a future therapeutic option for the treatment and prophylaxis of H1N1 viral infections.

Keywords: H1N1; neuraminidase; chalcone; molecular docking; NMR; antiviral activity; neuraminidase inhibition assay

Introduction

Influenza, an infectious disease caused by RNA viruses of the family *Orthomyxoviridae* (Colman *et al.,* 1989), attributes to significant morbidity and mortality. There are three types of influenza – A, B and C, where A is more prevalent as well as virulent (Hay *et al.,* 2001). Hemagglutinin (HA) and

neuraminidase (NA) are the two large glycoproteins on the outside surface of the viral particles. HA binds to the terminal sialic acid of the receptor and therefore is responsible for the entry of the viral genome into the target cell. NA cleaves the sialic acid that binds the mature viral particles by digesting it and therefore is responsible for the release of progeny virus from infected cells (Palese *et al.,* 1974; Liu *et al.,* 1995). Thus, inhibition of NA suppresses the viral growth by delaying the release of progeny virus from the surface of infected cells. In view of this, NA has become an attractive target for developing drugs against the influenza virus (De Clercq, 2006). Influenza A viruses are further classified into subtypes based on antibody responses to HA and NA. There are sixteen HA (H1 to H16) and nine NA (N1 to N9)

---

*Corresponding author. E-mail: meenatul@gmail.com; phone: +91-22-22164368, +91-22-22164387.
Abbreviations: DPPC = L-α-dipalmitoyl phosphatidyl choline; DS = discovery studio; HA = hemagglutinin; MLV = multilamellar vesicle; NA = neuraminidase; NMR = nuclear magnetic resonance

subtypes known, but only H 1-3, and N 1-2 are commonly found in humans (Organization, 1980). Vaccination or antiviral drug therapy are the two current ways to reduce the impact of influenza. Two classes of anti-influenza drugs for the treatment of influenza viruses are: the M2 proton channel inhibitors, viz. "entry inhibitors", and the NA inhibitors, viz. "release inhibitors". The M2 ion channel inhibitors' efficacies against influenza A virus are restricted due to occurrence of resistance towards it (Hayden and Couch, 1992; Moscona, 2005). NA inhibitors, like commercially available drugs zanamivir (ZMV) and oseltamivir (OMV), which are transition state analogues of sialic acid, inhibit NA, thereby inhibiting cleavage of the sialic acid and newly formed virion, which consequently inhibits further binding of HA and eventually its ability to promote attachment and fusion of the cell membrane to the virus (Greengard *et al.,* 2000; Porotto *et al.,* 2004). The interference with this process would likely interfere with also cell-cell fusion and virus entry step. It has been reported that influenza virus with NA subtype N1 is resistant to oseltamivir due to mutations, which are:

(1) His274Tyr; (2) Asn294Ser; and (3) a variant of N1 in which the generally conserved tyrosine residue at position 252 was replaced by histidine (Tyr252His) (Collins *et al.,* 2008). Similarly, zanamivir resistance has been associated with mutation of Gln136Lys, which breaks down bonding network formed by Asp151 and Arg156, leading to increased mobility of both groups (Hurt *et al.,* 2009). Reports indicate that natural compounds from plant sources are abundant with chalcones (1, 3-diphenyl-prop-2-ene-1-one) (Dao *et al.,* 2011). They are reported as non-competitive inhibitors of H1N1-NA (Dao *et al.,* 2010; Ryu, *et al.,* 2010; Nguyen *et al.,* 2011). We have focused on this scaffold as it has a structure different than the transition state analogue of endogenous ligand sialic acid. Our previous studies indicated that 2'-hydroxy-4-methoxy chalcone was a promising molecule, when evaluated using cell-based technique, in H1N1-NA inhibition (Pradip *et al.,* 2016). To understand the effect of additional hydroxy group and another polar amino group on anti-influenza activity, we have further developed a series of derivatives by introducing additional hydroxy group as in
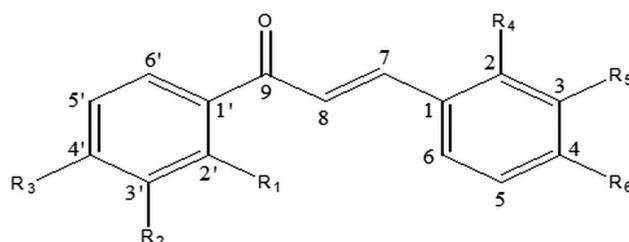
Sr. No.	Derivatives	R_1	R_2	R_3	R_4	R_5	R_6
01	A	NH_2	H	H	H	H	Cl
02	B	NH_2	H	H	H	Cl	H
03	C	NH_2	H	H	H	H	OCH_3
04	D	NH_2	H	H	H	H	NO_2
05	E	NH_2	H	H	Cl	H	H
06	F	NH_2	H	H	H	OCH_3	H
07	G	NH_2	H	H	H	NO_2	H
08	H	OH	H	OH	H	H	OCH_3
09	I	OH	H	OH	H	Cl	H
10	J	OH	H	OH	H	H	NO_2
11	K	OH	H	OH	H	OCH_3	H
12	L	H	NH_2	H	H	H	OCH_3
13	M	H	NH_2	H	H	H	NO_2
14	N	H	NH_2	H	H	NO_2	H

Fig. 1

General structure of chalcone (1, 3-diphenylprop-2-en-1-one) and various synthesized derivatives of chalcones with respective substituents

case of 2', 4'-dihydroxy chalcones and by introducing amino group at 2' and 3' positions. The other ring of the chalcone was substituted with electron-withdrawing and electron-donating groups, shown in Fig. 1, and evaluated by virtual screening, initially using molecular docking studies.

The binding interactions of chalcone derivatives with NA enzyme considering both seasonal as well as pandemic influenza virus (PDB codes 3B7E and 3TI6 respectively) were studied by molecular docking. The results were compared with docked marketed NA inhibitors oseltamivir and zanamivir, which were considered as standard drugs. Based on docking results, selective derivatives were synthesized and evaluated by *in vitro* enzyme-based antiviral studies (NA inhibition assay) on influenza A/Pune isolate/2009 (H1N1) virus. Additionally, we have also carried out ^{31}P NMR studies on our synthesized derivatives. We have investigated their general implications on phase behavior and structure architecture of L-α-dipalmitoyl phosphatidyl choline (DPPC) bilayer, which mimics biological membranes. The results of interaction studies further confirmed the membrane-stabilizing effect produced by our compounds, which is characteristics of antiviral drugs and is discussed later.

Materials and Methods

Materials. 2, 4-Dihydroxy acetophenone, 2-amino acetophenone, 3-amino acetophenone and substituted benzaldehyde were purchased from S D fine-chem. Ltd., India. All other solvents used for synthesis were of LR grade. DPPC was purchased from Sigma Chemicals Co., USA. Oseltamivir carboxylate was purchased from Clearsynth Labs Ltd., Mumbai, India. Oseltamivir phosphate was a gift sample from Cipla Ltd., India. The influenza A/Pune isolate/2009 (H1N1) virus was obtained from National Institute of Virology, Pune, India. Madin-Darby Cannine Kindey (MDCK)

cells obtained from National Centre for Disease Control (NCDC), Nasik, India.

Computational studies. Computational studies were carried out with the modeling package Discovery Studio *v* 3.1 (DS 3.1), Accelrys Inc., USA running on a Red Hat Enterprise platform. Docking studies were carried out with GOLD *v* 5.0.1, CCDC, UK running on a separate CentOS platform Linux Workstation.

Preparation of enzyme and ligand for docking. The X-ray crystal structure of the enzyme H1N1-NA in complex with zanamivir was taken from the protein data bank (PDB code no. 3B7E), which represents seasonal enzyme (Xu *et al.*, 2008). Similarly, X-ray crystal structure of the enzyme H1N1-NA in complex with oseltamivir was taken (PDB code No. 3TI6), which represents pandemic enzyme (Vavricka *et al.*, 2011). Monomeric unit of the dimeric enzyme was used for docking studies. The crystallographic waters were removed, hydrogen atoms were added, atom types and partial charges were assigned based on the CHARMm forcefield. Formal charges for the acidic and basic amino acids were set according to the physiological conditions at pH 7.4. N- and C-termini were capped with acetyl (ACE) and N-methyl-amino groups, respectively. The system was refined using the CHARMm forcefield to a gradient of 0.1 kcal/mol/Å. The oseltamivir, zanamivir and designed ligand structures were energy minimized using the "Smart Minimizer" method in energy minimization with the CHARMm forcefield to a gradient of 0.01 kcal/mol/Å. The docked poses were scored using GoldScore. The non-bonded interaction energy calculations contributed by van-der-Waals and Electrostatic energies were done by using "Simulation" module of DS 3.1 (Accelrys Inc., USA) running on a Red Hat Enterprise platform.

Docking protocol. The parameters in GOLD, kept similar as in our previously published work (Pradip *et al.*, 2016). The receptor active site was shaped by residues in a 10 Å vicinity of ligands OMV and ZMV. At the start of a docking run, all the variables were randomized in order to validate the protocol. Docking of OMV and ZMV was carried out for 20 genetic algorithm (GA) runs, which
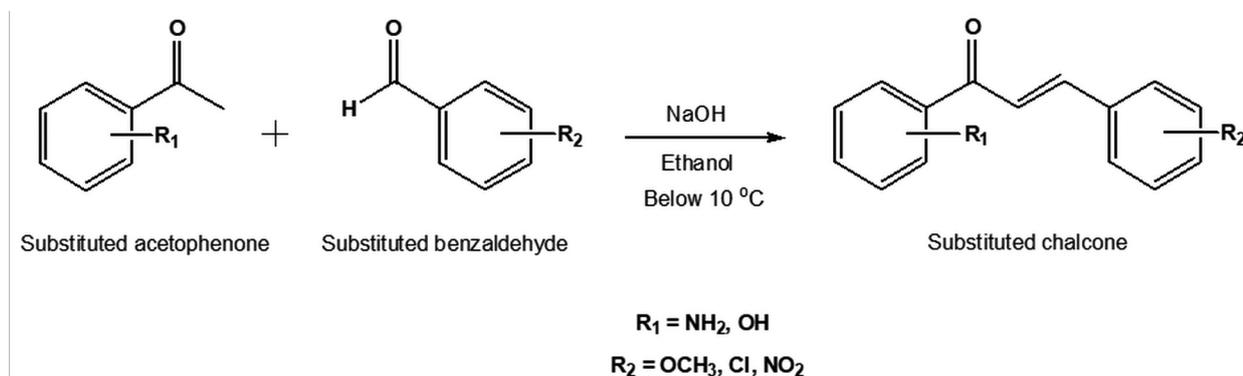

Fig. 2

Scheme of synthesis of chalcone derivatives by Claisen-Schmidt condensation reaction

was found sufficient to reproduce the binding pose of ZMV in PDB 3B7E and OMV in PDB 3TI6. The validated protocol was used to dock the designed chalcone derivatives in H1N1 to determine their preferred binding orientations.

Synthesis of chalcone derivatives. Based on docking results, H-bond interactions and non-bonded interaction energies (van-der-Waals and electrostatic energies, table not shown), we have selected and synthesized nine derivatives of chalcone, which showed prominent binding interactions with amino acid residues of NA active site. The synthesis is carried out based on Claisen-Schmidt condensation reaction. The schematic representation is shown in Fig. 2. As per the scheme, to a stirred mixture of 2/3/4-substituted acetophenone (1 mol) and 2/3/4-substituted benzaldehydes (1 mol) in absolute ethanol (5 ml), 10 ml of 20% solution of sodium hydroxide (NaOH) was added dropwise. The temperature was maintained below 10 ºC throughout the addition. The reaction mixture was stirred for 4 h at room temperature. The reaction mixture then was neutralized using concentrated hydrochloric acid (conc. HCl). The precipitate obtained was filtered and recrystallized using absolute ethanol (Vogel, Ed.5). The reactions were monitored by Thin Layer Chromatography. The structures of the synthesized compounds were characterized by proton nuclear magnetic resonance spectroscopy (^{1}H NMR) and infrared spectroscopy (IR) (figure not shown), which are summarized in Supplementary Table 1. NMR experiments were recorded on a 500 and 700 MHz BRUKER AVANCE NMR spectrometer and data was processed by using Bruker Topspin 2.1 software. In 1D proton NMR, 64 scans were recorded. 2D COSY (Correlation Spectroscopy) of the derivatives was recorded using standard pulse program and was used for structural elucidation (figure not shown).

Cells and virus. Madin-Darby Canine Kidney (MDCK) cells were grown in minimum essential medium (MEM, Gibco, by Life Technologies) supplemented with 10% fetal bovine serum (FBS, Gibco, by Life Technologies), 1% PenStrep (100 U/ml Penicillin and 0.5 mg/ml Streptomycin) (Hi-Media Laboratories, India). The influenza A/Pune isolate/2009 (H1N1) virus was propagated in MDCK cells in the presence of 2 µg/ml TPCK-trypsin.

Cytotoxicity studies. Cytotoxicity studies of the candidate molecules and standard drug (OMV) were carried out by MTT-Formazan assay. MDCK cells were seeded into 96-well plates and incubated at 37ºC with 5% CO_2 for 24 h until grown to 90% confluence. The plates were replaced with serum-free DMEM containing serially diluted compounds (1000–0.1 µmol/l). After 16 h of incubation, the medium was removed and 100 µl of a 0.5 mg/mL MTT (3-(4,5-dimethylthiozol-2-yl)-3,5-dipheryl tetrazolium bromide, Sigma-Aldrich), solution was added to each well and incubated at 37 ºC for 4 h. After removal of supernatant, 100 µl of dimethylsulfoxide (DMSO, Sigma-Aldrich) was added to each well to dissolve the formazan crystals. Absorbance was measured at 540 nm in a microplate reader (BioTek, Synergy HT) (Jeong, *et al.,* 2009). Data were normalized following the equation: Cell viability (%) = (sample value – blank control)/(cell control – blank control) x 100. A dose response curve was obtained using a non-

linear regression (curve fit), and the cytotoxic concentration 50% (CC_{50}) was calculated as the concentration required to reduce cell viability by 50%.

Neuraminidase inhibition assay. The anti-influenza activity of these compounds was further evaluated by enzyme-based neuraminidase inhibition assay. It was determined by the NA-Star Influenza Neuraminidase Inhibitor Resistance Detection Kit (Applied Biosystems, Foster City, CA) on influenza A H1N1 neuraminidase. Oseltamivir carboxylate (OMVC), as mentioned in the literature, was used as a standard. Briefly, 25 µl of half-log dilutions (0.03 to 1000 nmol/l) of synthesized compounds and OMVC were added in duplicates to the specified wells from column 1 through 10 in a 96-well microtiter plate. 25 µl of NA-Star assay buffer was added to control wells (negative control) without neuraminidase inhibitor to column 11 and 12. Also, 25 µl of diluted virus sample, viz. sH1N1 NA (1 ng/ml), per well was added in duplicates in column 1 through 11 and was mixed well by pipetting, while to the last column 25 µl of the uninfected culture supernatant diluted in NA-Star assay buffer was added. The plate was then incubated at 37ºC for 20 min. Further, the NA-Star substrate was diluted at 1:1000 in assay buffer immediately before use. Then, 10 µl of the diluted substrate was added to each well and mixed well by pipetting. The reaction mixtures were incubated at room temperature for 15 min. Further, the reaction mixtures were activated by adding 60 µl of NA-Star accelerator and the chemiluminescence signal was quantified immediately by microplate reader. The readings were taken within 5 min. after injection of accelerator. For measuring the chemiluminescence signal, the software was set at the readout time as 1 s/well with the delay of 2 s/well. The 50% inhibitory concentration (IC_{50}) was determined by regression analysis (Prism; version 6.00; GraphPad Software) (Gohil, *et al.,* 2015).

Drug-lipid interaction studies by determining Multilamellar Vesicles (MLV)-drug binding. For determination of drug-lipid binding, binding constants were determined by the centrifugation method as discussed in our previous work (Pradip *et al.,* 2016). The drug-liposome apparent binding constant (K) was analyzed using the double reciprocal plot. A plot of 1/(fraction bound) vs. 1/(lipid concentration) yields a straight line with slope 1/K.

Drug-lipid interaction studies using NMR (^{31}P NMR). For ^{31}P NMR study, MLVs were prepared by the standard procedure, also discussed in our previous work (Pradip *et al.,* 2016). ^{31}P NMR experiments were carried out at 323K with a relaxation delay of 1 s with broadband proton decoupling on MLVs of the sample (Aue *et al.,* 1976; Jeener *et al.,* 1979; Bothner-By *et al.,* 1984).

Results and Discussion

Docking

The initial validation studies with the docking protocol could satisfactorily reproduce (RMSD 0.5176 and 0.5512) the binding conformation of the ligand ZMV in the H1N1-
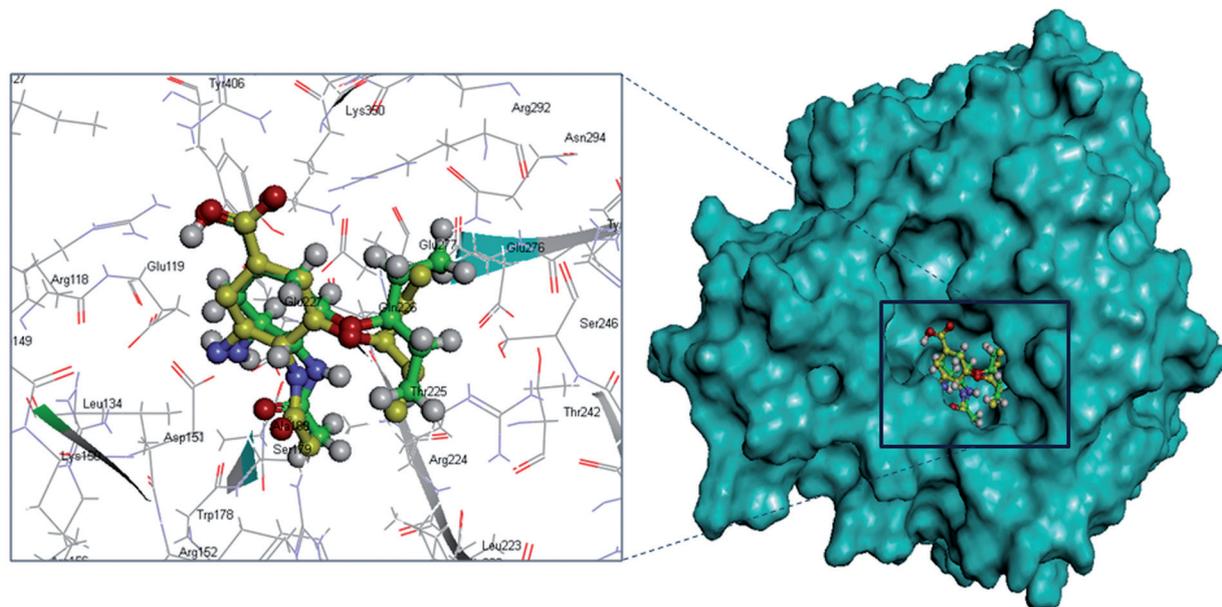
Fig. 3

Control docking of 3TI6, RMSD = 0.5512 Å. Superimposition of the docked and crystallographic oseltamivir poses (green and yellow, respectively) showing that the interacting residues are identical for both poses

NA crystal structure 3B7E and OMV in 3TI6, respectively, as shown in Fig. 3 (shown for OMV in 3TI6). All the interactions are consistent with original crystal structure of ZMV and OMV in PDB code 3B7E and 3TI6, respectively. The hydrogen bonding interactions and molecular surface model of oseltamivir and zanamivir in 3B7E and 3TI6 are depicted in Supplementary Fig. S1. The result emphasises the proper molecular volume, shape and electronic charge with respect to oseltamivir, which is critical for activity (D'Souza *et al.,* 2009). There are four well-conserved binding sites in H1N1-NA active site, which was discussed in our previous work, (Pradip, *et al.,* 2016) with 11 functional residues, which participate in the catalytic reaction (Colman, *et al.,* 1983). These are the positively charged site-1 (Arg118, Arg292 and Arg371), the negatively charged site-2 (Glu119, Glu227 and Asp151), site-3 (Ile222 and Tyr178), and site-4 (Glu276 and Glu277). Moreover, presence of the 150-loop (residues 147–152), that exists in two stable conformations (closed and open), forms one part of the enzyme active site. It was reported that initially oseltamivir binds to "open" form of NA. Subsequently, it changes into "closed" form by undergoing a conformational change (Chintakrindi *et al.,* 2012). Interestingly, the crystal structure of NA from the 2009 pandemic H1N1 influenza strain indicates that it lacks the 150-loop in its active site (similar to closed conformation). This indicates importance of open and closed conformations of 150-loop in the design of newer NA inhibitors. Further, literature survey

(Varghese *et al.,* 1998; Reece, 2007) on molecular modeling studies of OMV, unlike ZMV, indicates that the neuraminidase molecule undergoes rearrangement to create an additional binding pocket to accommodate the hydrophobic side chain of oseltamivir in the active site. The binding pocket is formed when the amino acid Glu276 rotates due to ionic interaction with Arg224 and binds with it. However, the ionic interaction between Glu276 and Arg224 is prevented owing to the mutations Arg292Lys, Asn294Ser, and His274Tyr, due to which the rotation of Glu276 is inhibited.

The hydrogen bonding interactions and molecular surface model of chalcone derivatives with NA active site in 3B7E and 3TI6 are depicted in Fig. 4 and 5, respectively. The hydrogen bonds formed between the substrate/inhibitors and the enzyme are summarized in Supplementary table 2 for 3B7E and Supplementary table 3 for 3TI6. Docking studies of all the chalcone derivatives with both seasonal and pandemic virus revealed that they occupied site-1 as that observed with OMV, while showed different preferences for interaction at other sites based on their structural variations. Interestingly, the designed chalcone derivatives showed binding poses, which were not similar to either standard NA inhibitors or endogenous ligand. This finding might highlight mutual non-competitive nature of the designed chalcone molecules as they showed binding in the same catalytic cavity but different interactions than the standard drugs or endogenous ligand. In docking studies of 2', 4'-Dihydroxy series with

seasonal enzyme revealed that though 1A fitted well into the cavity, it showed interactions quite different from that of oseltamivir. When compared with 1A, the other derivatives 1B, 1C and 1D do not fit as well into the cavity of the seasonal enzyme as 1A. But they showed better fit into the cavity of the pandemic enzyme. Thus, these derivatives might have better activity in the pandemic enzyme. It was observed that in 2'-Amino series, although 2A virtually fitted in the same NA cavity (both seasonal and pandemic) in a similar pose as 2C, it lacked the interaction with Arg224. Also, it was observed that in pandemic enzyme, 2B showed additional interaction with Arg224. This interaction might facilitate further rotation of Glu276 in order to accommodate 4-chloro group and reorient itself to form additional pocket. In case of 2D, bumping of 4-nitro was observed to the receptor surface of both seasonal and pandemic enzyme. This might be because of prominent electronic effect of nitro group in 2D as compared with other derivatives. Consequently, this bumping might have changed its overall interactions, preventing its access

to the receptor cavity. This might be attributed to its lesser NA inhibition activity, which is discussed later.

Chemistry

In the ^{1}H NMR spectra of chalcones olefinic protons H-α and H-β appeared as doublets in the range of δ 7.0–7.77 and δ 7.7–8.2, respectively. The coupling constant of vinyl hydrogen (15.5±1 Hz) confirmed the trans-stereochemistry of enone moiety of synthesized chalcones. The IR spectra of chalcones showed carbonyl absorption in the range of 1639.49–1708.81 cm^{-1} and an olefinic C=C in the range 1519.58–1612.49 cm^{-1}.

Antiviral evaluation

No tested compounds showed any significant cytotoxicity except for 2A, 2B, 2D and 3A, which showed CC_{50} value >100 μmol/l. CC_{50} values are indicated in Table 1. Our
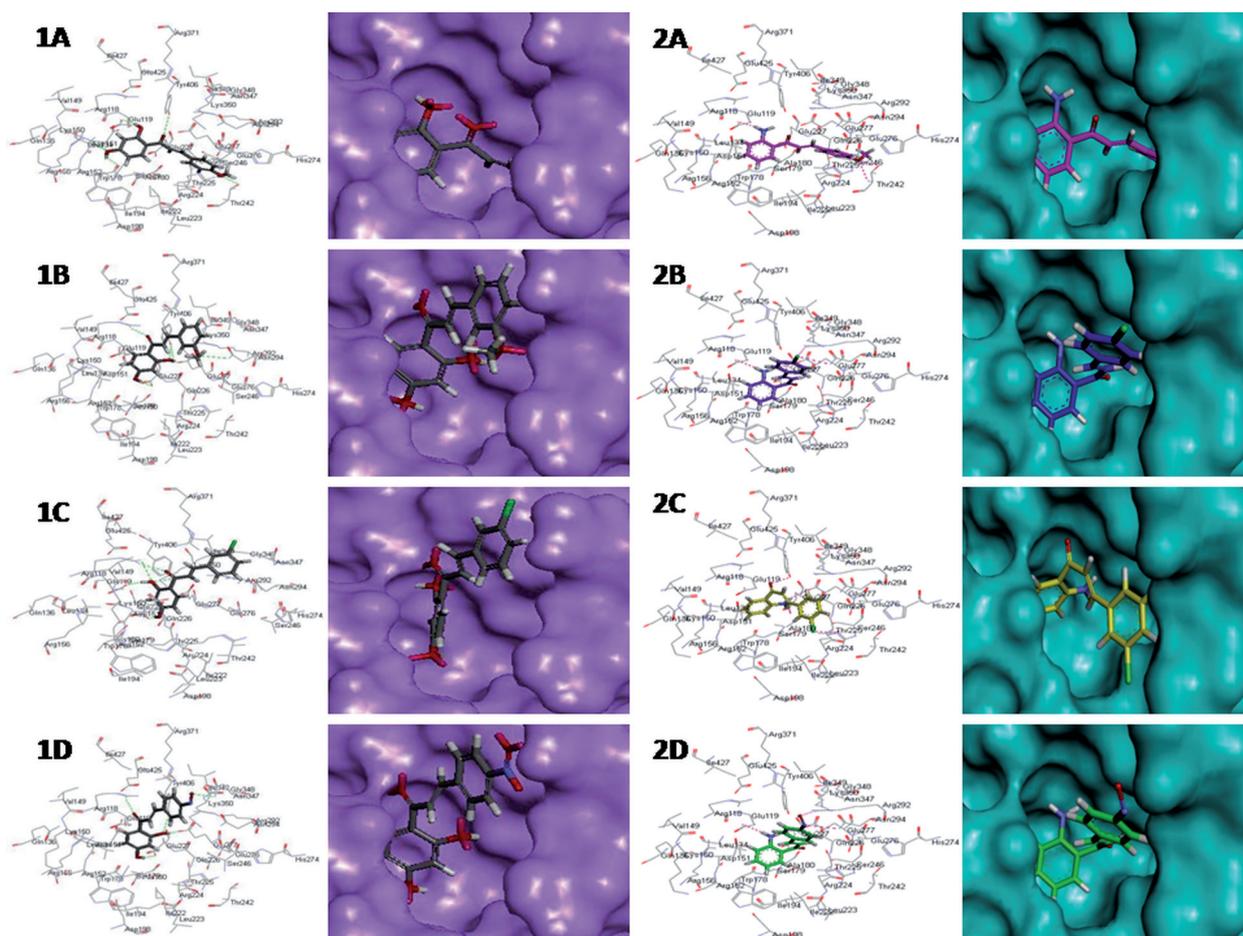
Fig. 4

Hydrogen bonding and molecular surface models of chalcone derivatives with NA active site of seasonal 3B7E protein
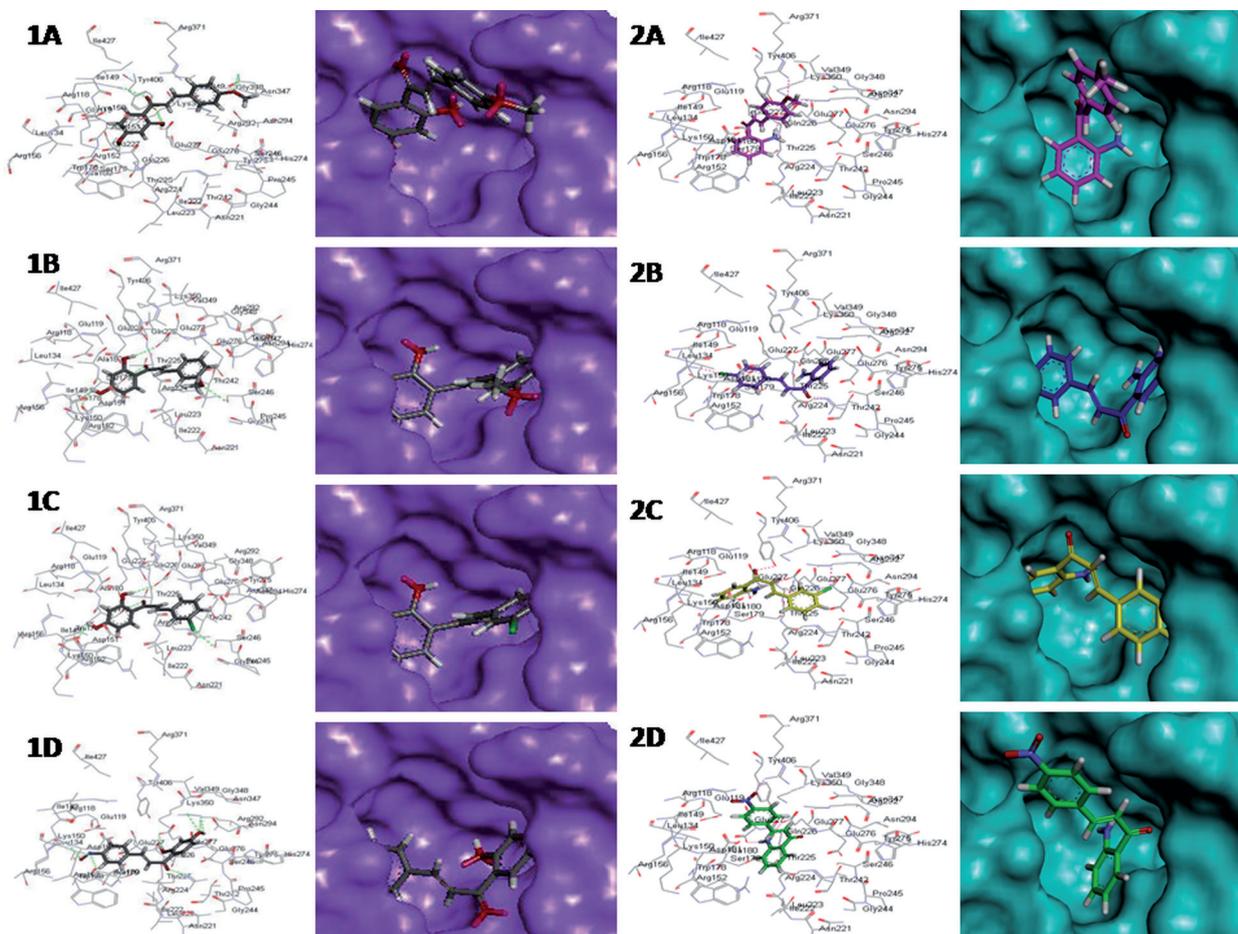
Fig. 5

Hydrogen bonding and molecular surface models of chalcone derivatives with NA active site of pandemic 3TI6 protein

Table 1. *In vitro* evaluation of tested compounds

Code	Compound	CC_{50} (µmol/l)	IC_{50} (µmol/l)	SI[*]
1A	2', 4'-dihydroxy-4-methoxy chalcone	>500	2.23	>224.2
1B	2', 4'-dihydroxy-3-methoxy chalcone	>500	8.71	>57.4
1C	2', 4'-dihydroxy-3-chloro chalcone	>250	3.58	>69.8
1D	2', 4'-dihydroxy-4-nitro chalcone	>125	6.64	>18.8
2A	2'-amino-4-methoxy chalcone	>100	47.864	>2.1
2B	2'-amino-4-chloro chalcone	>100	15.041	>6.6
2C	2'-amino-3-chloro chalcone	>125	32.656	>3.8
2D	2'-amino-4-nitro chalcone	>100	52.651	>1.9
3A	3'-amino-4-methoxy chalcone	>100	41.1	>2.4
OMVC	oseltamivir carboxylate	>1000	7×10^{-3}	$>447.02 \times 10^{-3}$

All compounds were examined in a set of triplicate experiments for cytotoxicity study and duplicate experiments for NA inhibition assay; SI = Selectivity Index was generated by the ratio of CC_{50} and IC_{50}; CC_{50} values of compounds represent the concentration that caused 50% reduction in cell viability; IC_{50} values of compounds represent the concentration that caused 50% enzyme activity loss.

previous studies indicated that the 2'-hydroxy-4-methoxy derivative of chalcone synthesized by us showed EC_{50} value at 3.54 nmol/l (whereas oseltamivir phosphate as stand-ard showed EC_{50} value at 7.1 nmol/l) when evaluated by cell-based assay (hemagglutination assay) indicating good antiviral activity (Pradip *et al.,* 2016). In the current work,

where enzyme-based assay was performed using NA-star kit, the same derivative showed IC_{50} value at 7.57 µmol/l, where standard drug oseltamivir carboxylate (OMVC) showed IC_{50} value at 2.23 nmol/l. When one more hydroxy group was introduced to 2'-Hydroxy series, the activity was improved (1A showed NA inhibition i.e. IC_{50} value at 2.23 µmol/l). But replacing 2'-hydroxy with 2'-amino and 3'-amino groups decreased the activity. The IC_{50} values for tested chalcone derivatives are depicted in Table 1 and dose-response curves of tested chalcone derivatives and OMVC are depicted in Fig. 6.

Drug-lipid interaction studies

The efficiency of drugs to interact with the membranes constitutes one of the most important pharmacological features playing an essential role in their biological activity.

Although drugs bind to proteins and regulate their activity, their interaction with the membrane lipid phase is equally important. The structural changes induced by the drug in lipid phase might change membrane function and consecutively modulate membrane proteins. In this context, we have conducted the drug-lipid binding studies using centrifugation method and drug-lipid interaction studies using NMR spectroscopy specifically, ^{31}P NMR.

Drug-lipid binding studies

For all candidate molecules under study, an increase in binding affinity was observed with increasing concentration of lipid. All selected derivatives showed nearly 60% to 70% of binding to the lipid even at a relatively low concentration of lipid. Double inverse plot of fraction of drug bound vs. inverse of lipid concentration had been
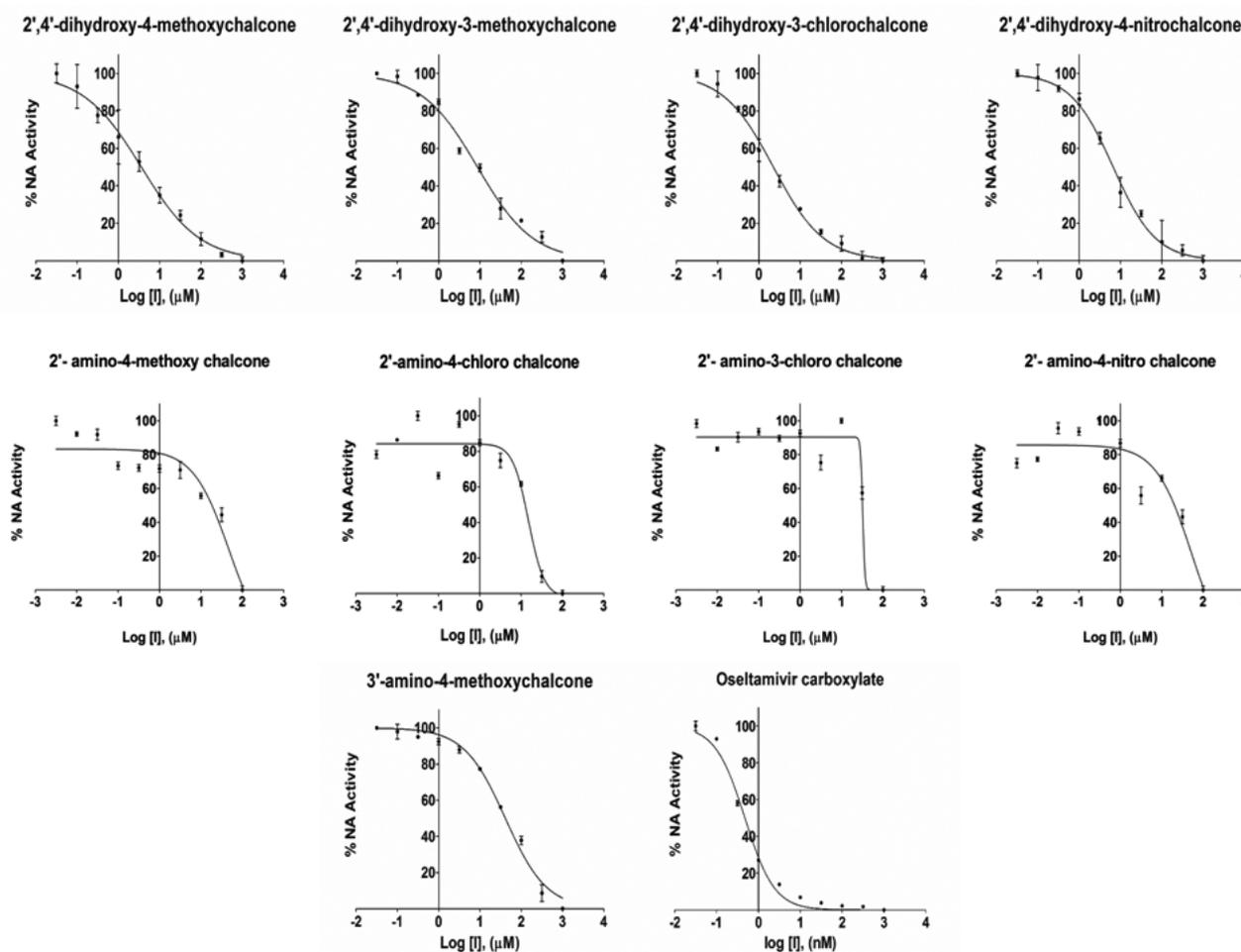
Fig. 6

Dose-response curve (H1N1 percentage inhibition versus Log_{10} concentration) of tested chalcone derivatives and OMVC, indicating effects of tested compounds on H1N1-NA for the hydrolysis of substrate

used to calculate the binding constants (data not shown). The results indicated that these molecules bind to the multilamellar vesicles (MLV) of lipid with a variable degree of affinity. The apparent binding constants measured for 2′, 4′-dihydroxy chalcone derivatives were: 1A = 0.4629 M^{-1}, 1B = 0.6944 M^{-1}, 1C = 0.8621 M^{-1}, 1D = 0.0961 M^{-1} and for 2′-amino chalcone derivatives were: 2A = 0.7320 M^{-1}, 2B = 1.1248 M^{-1}, 2C = 0.8237 M^{-1} and 2D = 0.5934 M^{-1}. The order of binding for 2′, 4′-dihydroxy chalcone derivatives was 1C (3-chloro) > 1B (3-methoxy) > 1A (4-methoxy) > 1D (4-nitro) and that for 2′-amino chalcone derivatives was 2B (4-chloro) > 2C (3-chloro) > 2A (4-methoxy) > 2D (4-nitro). The variation in the measured binding constants of the candidate molecules was attributed to the electronic and steric properties of the substituents on hydrophilicity/hydrophobicity. The above observations of MLV-drug binding studies indicated that our chalcone derivatives used their hydrophobic aromatic ring and polar group to bind with the lipid spanning both interior as well as the head group of the lipid bilayer.

^{31}P NMR

In order to understand the intermolecular interaction between derivatives and the lipid membrane, ^{31}P NMR experiments had been carried out for our synthesized chalcone derivatives in presence of the lipid bilayers of DPPC that serves as model membrane. ^{31}P NMR spectroscopy is widely used for studies of phospholipid bilayers and biological membranes in native conditions. The analysis of ^{31}P NMR spectra of lipids could provide a wide range of information about lipid bilayer packing, phase transitions, lipid head group orientation/dynamics, and elastic properties of pure lipid bilayer in native state and after binding with proteins and other biomolecules (Chary and Govil, 2008). Lipid bilayers give a characteristic broad spectrum with a high field peak and low field ^{31}P line
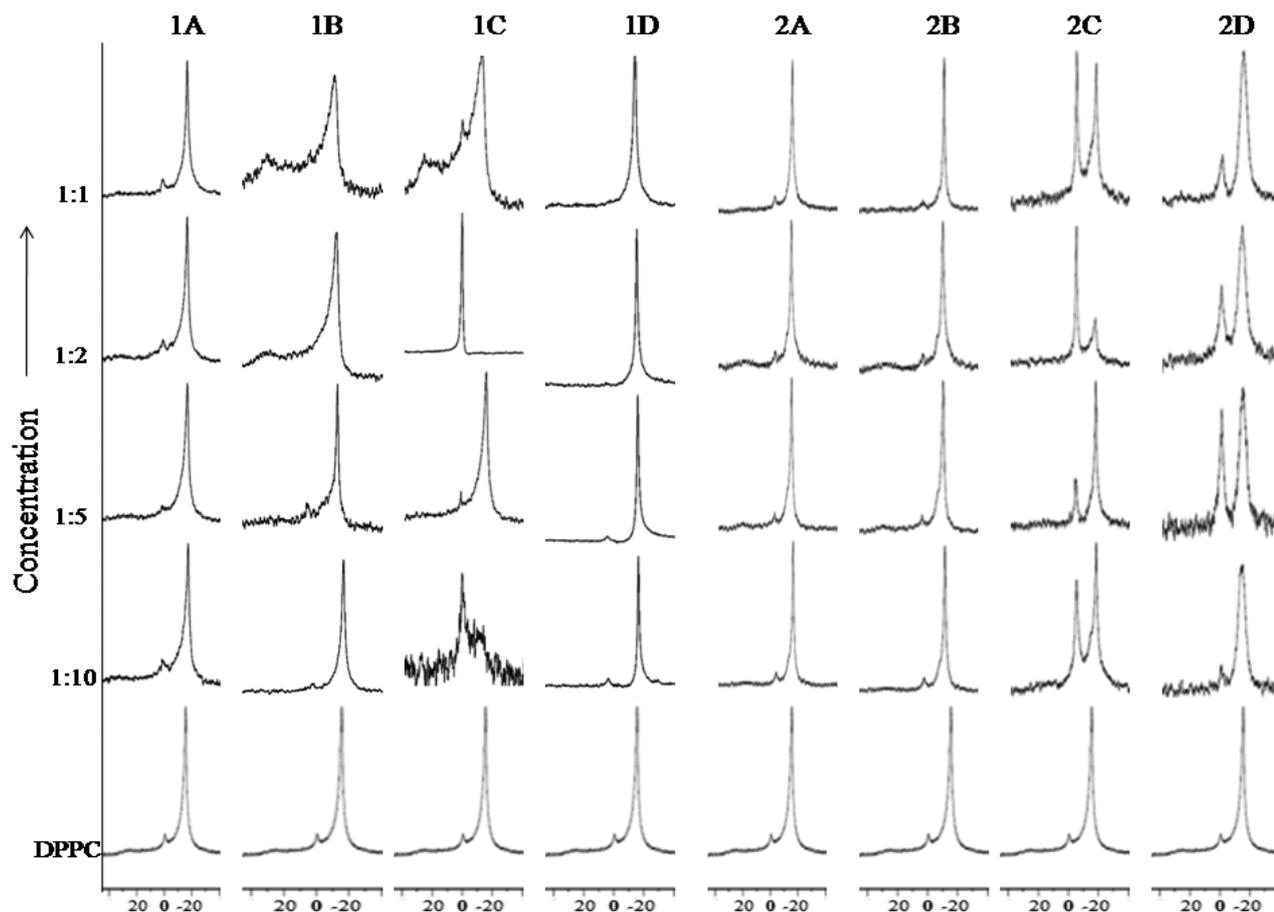
Fig. 7

500 MHz concentration dependent ^{31}P NMR spectra of DPPC (100 mmol/l) multilamellar vesicles incorporated with chalcone derivatives
The additives: lipid molar ratios are **(A)** 0:100, **(B)** 1:5, **(C)** 1:2, and **(D)** 1:1. All experiments are at 323 K.

shoulder. The ^{31}P NMR resonance line shape was determined by the chemical shift anisotropy (CSA) (measured from the low $\sigma_{\parallel}$ and high $\sigma_{\perp}$ field shoulders of the spectrum, $\Delta\sigma = \sigma_{\perp} - \sigma_{\parallel}$) of the phosphate group coupled with the molecular motions near the bilayer head groups (Srivastava *et al.*, 1988).

The change in ^{31}P NMR line shape of lipid bilayers incorporated with increasing concentrations of chalcone derivatives is showed in Fig. 7. In each case, the lower most graphs represent the ^{31}P NMR line shape for lipid bilayers alone (Fig. 7. DPPC). In a randomly oriented sample such as DPPC dispersions in the gel phase, the overall rotational rate is slow. One observes a sharp signal at -20 ppm from lipid molecules with their long axis oriented perpendicular to the direction of the magnetic field ($\sigma_{\perp}$), while for the parallel alignment of the lipid molecules ($\sigma_{\parallel}$) a broad shoulder appears at 25 ppm. A relatively small but sharp peak is observed at 0 ppm due to the formation of a small amount of unilamellar vesicles with a small size that permits fast internal and tumbling motions. It may be noted here that these molecules do not alter the characteristic line shapes exhibiting bilayer features of the MLV's of lipid at all concentrations.

In case of derivatives 1A, 1D, 2A and 2B, ^{31}P line shape was not affected and remained very similar to DPPC. Though it was observed that the peak at 0 ppm broadened very slightly except for 1D, where it had completely broadened as the concentration of drug increased; still the bilayer feature remained intact (Fig. 7. 1A, 1D, 2A & 2B). The bilayer features remained intact to a large extent keeping the vesicles highly rigid. This suggested that derivatives 1A, 1D, 2A and 2B imparted very little perturbation to the bilayer. In case of derivative 1B, with increasing concentration, the peak at 0 ppm became broad. The perpendicular peak (-20 ppm) in this case remained unaffected though the intensity reduced as the drug concentration increased (Fig. 7. 1B). This indicated that there is slight perturbation of the lipid bilayer structure as the drug concentration was increased. In case of 3-Chloro derivative of both hydroxy and amino series (i.e. 1C and 2C), it was observed that the ^{31}P line shape changed as the concentration of the drug varied. At the drug:lipid molar ratio of 1:10 for 1C and; 1:2 and 1:1 for 2C, the 0 ppm peak was at a greater intensity than the perpendicular peak (Fig. 7. 1C and 2C). This indicated the possibility of the drug to accommodate itself in the lipid bilayer, leading to transformation of original multilamellar bilayer phase. But the perpendicular peak did not completely disappear, indicating that there was membrane-stabilizing effect. In case of derivative 2D, the peak at 0 ppm became sharper and increased in intensity at higher concentration (1:5). The perpendicular peak showed no change in intensity, but it showed sufficient amount of broadening at lower concentrations (1:10 and 1:5) (Fig. 7. 2D). This suggested that multilamellar bilayer phase was slightly disrupted, which might be due to formation of smaller-size vesicles. Overall results indicated that derivative 2D imparted very little perturbation to the bilayer.

Consequently, all the above observations of ^{31}P NMR studies done on our candidate molecules indicated that all the derivatives showed membrane stabilizing effect. Literature survey on cyclosporine A and other antiviral drugs have shown that stabilization of the membrane by antiviral drugs can play an important role in inhibiting membrane fusion and also antiviral activity (Epand *et al.*, 1987; McKenzie *et al.*, 1987). Our chalcone derivatives, therefore, seemed to be involved in preventing membrane fusion in addition to inhibition of NA activity.

Conclusion

With the above findings, we conclude that based on our previous studies, which indicated that 2'-hydroxy-4-methoxy chalcone was a promising candidate as per its EC_{50} value, here we have studied the effect of inserting an additional hydroxy group as well as replacement of hydroxy group with amino group of the chalcone molecule on the antiviral activity supported by molecular docking and membrane interaction studies using NMR. The most buoyant derivative 1A (2', 4'-dihydroxy-4-methoxy chalcone) can be explored further.

Supplementary information is available in the online version of the paper.

References

Discovery Studio version 3.1. USA: Accelrys Inc.

Aue WP, Bartholdi E, Ernst RR (1976): Two-dimensional spectroscopy. Application to nuclear magnetic resonance. J. Chem. Physics 64, 2229–2246. https://doi.org/10.1063/1.432450

Bothner-By, Aksel A, Stephens RL, Lee J, Warren CD, Jeanloz RW (1984): Structure determination of a tetrasaccharide: transient nuclear Overhauser effects in the rotating frame. J. Am. Chem. Soc 106, 811–813. https://doi.org/10.1021/ja00315a069

Chary KVR, Girjesh G (2008): NMR in biological systems: from molecules to human. Volume 6, Springer Science & Business Media. https://doi.org/10.1007/978-1-4020-6680-1

Chintakrindi A, D'Souza CH, Kanyalkar M (2012): Rational development of neuraminidase inhibitor as novel anti-flu drug. Mini-Rev. Med. Chem. 12, 1273–1281. https://doi.org/10.2174/138955712802761997

Collins PJ, Haire LF, Lin YP, Liu J, Russell RJ et al. (2008): Crystal structures of oseltamivir-resistant influenza virus neuraminidase mutants. Nature 453, 1258–1261. https://doi.org/10.1038/nature06956

Colman PM, Tulip WR, Varghese JN, Tulloch PA, Baker AT, Laver WG, Air GM, Webster RG (1989): Three-dimensional structures of influenza virus neuraminidase-antibody complexes. Philos. Trans. R. Soc. Lond. B Biol. Sci. 323 (0962–8436 (print)), 511–518. https://doi.org/10.1098/rstb.1989.0028

Colman PM, Varghese JN, Laver WG (1983): Structure of the catalytic and antigenic sites in. Nature 303, 41. https://doi.org/10.1038/303041a0

D'Souza CH, Kanyalkar M, Joshi M, Coutinho E, Srivastava S (2009): Search for novel neuraminidase inhibitors: Design, synthesis and interaction of oseltamivir derivatives with model membrane using docking, NMR and DSC methods. Biochim. Biophys. Acta 1788, 1740–1751. https://doi.org/10.1016/j.bbamem.2009.04.014

Dao TT, Tung BT, Nguyen PH, Thuong PT, Yoo SS, Kim EH, Kim SK, Oh WK (2010): C-Methylated Flavonoids from Cleistocalyx operculatus and Their Inhibitory Effects on Novel Influenza A (H1N1) Neuraminidase. J. Nat. Prod. 73, 1636–1642. https://doi.org/10.1021/np1002753

Dao TT, Nguyen PH, Lee HS, Kim EH, Park J, Lim SI, Oh WK (2011): Chalcones as novel influenza A (H1N1) neuraminidase inhibitors from Glycyrrhiza inflata. Bioorganic Med. Chem. Lett 21, 294–298. https://doi.org/10.1016/j.bmcl.2010.11.016

De Clercq E (2006): Antiviral agents active against influenza A viruses. Nat. Rev. Drug Discov. 5, 1015–1025. https://doi.org/10.1038/nrd2175

Epand RM, Epand RF, McKenzie RC (1987): Effects of viral chemotherapeutic agents on membrane properties. Studies of cyclosporin A, benzyloxycarbonyl-D-Phe-L-Phe-Gly and amantadine. J. Biol. Chem. 262, 1526–1529.

Gohil D, Kothari S, Shinde P, Chintakrindi AC, Meharunkar R, Warke R, Kanyalkar M, Chowdhary A, Deshmukh R (2015): Genetic characterization of oseltamivir-resistant seasonal influenza A (H1N1) virus circulating during 2009 pandemic influenza in Mumbai. Int. J. Adv. Res. 3, 252–261.

Greengard O, Poltoratskaia N, Leikina E, Zimmerberg J, Moscona A (2000): The Anti-Influenza Virus Agent 4-GU-DANA (Zanamivir) Inhibits Cell Fusion Mediated by Human Parainfluenza Virus and Influenza Virus HA. J. Virol. 74, 11108–11114. https://doi.org/10.1128/JVI.74.23.11108-11114.2000

Hay AJ, Gregory V, Douglas AR, Lin YP (2001): The evolution of human influenza viruses. Philos. Trans. R. Soc. Lond. B. Biol. Sci. 356, 1861–1870. https://doi.org/10.1098/rstb.2001.0999

Hayden FG, Couch RB (1992): Clinical and epidemiological importance of influenza a viruses resistant to amantadine and rimantadine. Rev. Med. Virol. 2, 89–96. https://doi.org/10.1002/rmv.1980020205

Hurt AC Holien JK, Parker M, Kelso A, Barr IG (2009): Zanamivir-Resistant Influenza Viruses with a Novel Neuraminidase Mutation. J. Virol. 83, 10366–10373. https://doi.org/10.1128/JVI.01200-09

Jeener J, Meier BH, Bachmann P, Ernst RR (1979): Investigation of exchange processes by two dimensional NMR spectroscopy. J. Chem. Phys. 71, 4546–4553. https://doi.org/10.1063/1.438208

Jeong HJ, Ryu YB, Park SJ, Kim JH, Kwon HJ et al. (2009): Neuraminidase inhibitory activities of flavonols isolated from Rhodiola rosea roots and their in vitro anti-influenza viral activities. Bioorganic Med. Chem. 17, 6816–6823. https://doi.org/10.1016/j.bmc.2009.08.036

Liu C, Eichelberger MC, Compans RW, Air GM (1995): Influenza type A virus neuraminidase does not play a role in viral entry, replication, assembly, or budding. J. Virol. 69, 1099–1106.

McKenzie RC, Epand RM, Johnson DC (1987): Cyclosporine A inhibits herpes simplex virus-induced cell fusion but not virus penetration into cells. Virology 159, 1–9. https://doi.org/10.1016/0042-6822(87)90341-2

Moscona A (2005): Oseltamivir Resistance-Disabling Our Influenza Defenses. N. Engl. J. Med. 353, 2633–2636. https://doi.org/10.1056/NEJMp058291

Nguyen TNA, Dao TT, Tung BT, Choi H, Kim E et al. (2011): Influenza A (H1N1) neuraminidase inhibitors from Vitis amurensis. Food Chem. 124, 437–443. https://doi.org/10.1016/j.foodchem.2010.06.049

Organization, World Health (1980): A revision of the system of nomenclature for influenza viruses: a WHO Memorandum. Bull. Wrld. Health Organ. 58, 585–591.

Palese P, Tobita K, Ueda M, Compans RW (1974): Characterization of temperature sensitive influenza virus mutants defective in neuraminidase. Virology 61, 397–410. https://doi.org/10.1016/0042-6822(74)90276-1

Porotto M, Murrell M, Greengard O, Lawrence MC, McKimm-Breschkin JL, Moscona A (2004): Inhibition of Parainfluenza Virus Type 3 and Newcastle Disease Virus Hemagglutinin-Neuraminidase Receptor Binding: Effect of Receptor Avidity and Steric Hindrance at the Inhibitor Binding Sites. J. Virol. 78, 13911–13919. https://doi.org/10.1128/JVI.78.24.13911-13919.2004

Pradip S, Khushboo M, Anand C, Devanshi G, Sudha S et al. (2016): Virucidal Activity of Newly Synthesized Chalcone Derivatives against H1N1 Virus Supported by Molecular Docking and Membrane Interaction Studies. J. Antiviral. Antiretroviral. 8, 079–089.

Reece PA (2007): Neuraminidase inhibitor resistance in influenza viruses. J. Med. Virol. 79, 1577–1586. https://doi.org/10.1002/jmv.20951

Ryu YB, Kim JH, Park SJ, Chang JS, Rho MC, Bae KH, Park KH, Lee WS (2010): Inhibition of neuraminidase activity by

polyphenol compounds isolated from the roots of Glycyrrhiza uralensis. Bioorganic Med. Chem. Lett. 20, 971–974. https://doi.org/10.1016/j.bmcl.2009.12.106

Srivastava SR, Phadke S, Govil G (1988): Role of tryptophan in inducing polymorphic phase formation in lipid dispersions. Indian J. Biochem. Biophys. 25, 283–286.

Varghese JN, Smith PW, Sollis SL, Blick TJ, Sahasrabudhe A et al. (1998): Drug design against a shifting target: a structural basis for resistance to inhibitors in a variant of influenza virus neuraminidase. Structure 6, 735–746. https://doi.org/10.1016/S0969-2126(98)00075-6

Vavricka CHJ, Li Q, Wu Y, Qi J, Wang M et al. (2011): Structural and Functional Analysis of Laninamivir and its Octanoate Prodrug Reveals Group Specific Mechanisms for Influenza NA Inhibition. PLoS Pathog. 7, 1002249–1002259. https://doi.org/10.1371/journal.ppat.1002249

Vogel's Text book of Practical Organic Chemistry. Ed.5, Bath Press, pp. 1034

Xu X, Zhu X, Dwek RA, Stevens J, Wilson IA (2008): Structural characterization of the 1918 influenza virus H1N1 neuraminidase. J. Virol. 82 1098–5514 (electronic), 10493–10501 (print).

Supplementary information

In search of effective H1N1 neuraminidase inhibitor by molecular docking, antiviral evaluation and membrane interaction studies using NMR

K. MALBARI[1], H. GONSALVES[1], A. CHINTAKRINDI[1], D. GOHIL[2], M. JOSHI[3], S. KOTHARI[2], S. SRIVASTAVA[3],
A. CHOWDHARY[2], M. KANYALKAR[1*]

[1]Department of Pharmaceutical Chemistry, Prin K. M. Kundnani College of Pharmacy, Plot 23, Jote Joy Building, Rambhau Salgaonkar
Marg, Cuffe Parade, Mumbai-400 005, India; [2]Haffkine Institute for Training, Research and Testing, Parel, Mumbai- 400 012, India;
[3]National Facility for High Field NMR, Tata Institute of Fundamental Research, Homi Bhabha Road, Colaba, Mumbai-400 005, India

Supplementary Fig. 1

The most favored poses of oseltamivir (green color) in 3B7E (a) and 3TI6 (b); and zanamivir (yellow color) in 3B7E (a') and 3TI6 (b') in the H1N1-NA active site as seen by docking studies. H-bonds between drugs and enzymes are indicated (pink).

Supplementary Table 1. Chemistry of synthesized chalcone derivatives

Code No.	Structure	IR		^{1}H NMR	
		Attributes	**Absorption range (cm$^-$)**	**Atom**	**Chemical shift (σ ppm)**
Derivative 1A (2′, 4′-Dihydroxy-4-methoxy chalcone)		OH Stretch	3361.02, 3465.89	OH	12.5 (s)
				OH	10.5 (bs)
		CH Stretch Alkene	3040.02	CH (7)	7.9 (d)
		C=O Stretch	1662.88	CH (2, 6, 6')	7.7 (d)
		α, β unsaturated		CH (3, 5, 8)	7.0 (d)
		C=C Stretch	1519.58	CH (5')	6.4 (d)
		Alkene and		CH (3')	6.2 (s)
		Aromatic		OCH$_3$ (4)	3.8 (s)
		O-CH$_3$ Stretch aromatic	1022.20		
Derivative 1B (2′, 4′-Dihydroxy-3-methoxy chalcone)		OH Stretch	3279.87	OH	12.5 (s)
		C=O Stretch	1687.60	OH	10.5 (bs)
		α, β unsaturated		CH (7, 6')	7.7 (d)
		C=C Stretch	1602.74	CH (8)	7.5 (d)
		Alkene and		CH (2)	7.48 (s)
		Aromatic		CH (5)	7.43-7.46 (t)
		O-CH$_3$ Stretch aromatic	1041.49	CH (6)	7.2 (d)
				CH (4, 5')	6.4 (d)
				CH (3')	6.2 (s)
				OCH$_3$ (3)	3.8 (s)
Derivative 1C (2′, 4′-Dihydroxy-3-chloro chalcone)		OH Stretch	3363.07, 3494.01	OH	12.5 (s)
				OH	10.5 (bs)
		C=O Stretch	1687.60	CH (2, 6, 7)	7.90-7.92 (s, d)
		α, β unsaturated		CH (6', 8)	7.77 (d)
		C=C Stretch	1600.56	CH (4)	7.71 (d)
		Alkene and		CH (5)	7.5 (t)
		Aromatic		CH (5')	6.4 (d)
		Cl Stretch	748.33	CH (3')	6.2 (s)

Code No.	Structure	IR		¹H NMR	
		Attributes	Absorption range (cm⁻)	Atom	Chemical shift (σ ppm)
Derivative 1D (2′, 4′-Dihydroxy-4-nitro chalcone)		OH Stretch	3520.04	OH	5.4 (s)
		CH Stretch Alkene	3080.32	CH (3, 5, 7)	8.2 (d)
		C=O Stretch	1708.81	CH (8, 6')	7.6 (d)
		α, β unsaturated		CH (2, 6, 5')	6.7 (d)
		C=C Stretch	1600.81	CH (3')	6.1 (s)
		Alkene and Aromatic			
		NO₂ Stretch aromatic	1338.51		
Derivative 2A (2′-Amino-4-methoxy chalcone)		NH₂ Stretch	3427.51	NH₂ (2')	7.3 (bs)
		CH Stretch Alkene	2918.30	CH (2, 6)	7.0 (d)
		C=O Stretch	1639.49	CH (3, 5, 7)	7.82 – 7.85 (d, d)
		α, β unsaturated			
		C=C Stretch	1612.49	CH (4)	3.8 (s)
		Alkene and Aromatic		CH (8)	7.6 (d)
				CH (3')	6.8 (d)
		O-CH₃ Stretch aromatic	1093.23	CH (4')	6.6 (t)
				CH (5')	7.3 (d)
				CH (6')	8.0 (d)
Derivative 2B (2′-Amino-4-chloro chalcone)		NH₂ Stretch	3302.13, 3466.08	NH₂ (2')	7.4 (bs)
				CH (2, 6)	7.9 (d)
		CH Stretch Alkene	3037.89	CH (3, 5)	7.5 (d)
		C=O Stretch	1645.28	CH (8)	7.6 (d)
		α, β unsaturated		CH (7)	7.9 (d)
		C=C Stretch	1610.56	CH (3')	6.8 (d)
		Alkene and Aromatic		CH (4')	6.6 (t)
				CH (5')	7.3 (d)
		Cl Stretch	754.17	CH (6')	8.1 (d)

Code No.	Structure	IR		^{1}H NMR	
		Attributes	Absorption range (cm$^-$)	Atom	Chemical shift (σ ppm)
Derivative 2C (2′-Amino-3-chloro chalcone)		NH$_2$ Stretch	3302.13, 3466.08	NH$_2$ (2')	7.4 (bs)
				CH (2)	7.8 (s)
		CH Stretch Alkene	3037.89	CH (4, 5)	7.49 – 7.50 (d, t)
		C=O Stretch	1645.28		
		α, β unsaturated		CH (6, 7)	8.05 – 8.07 (d, d)
		C=C Stretch	1610.56		
		Alkene and		CH (8)	7.6 (d)
		Aromatic		CH (3')	6.8 (d)
		Cl Stretch	754.17	CH (4')	6.6 (t)
				CH (5')	7.3 (d)
				CH (6')	8.1 (d)
Derivative 2D (2′-Amino-4-nitro chalcone)		NH$_2$ Stretch	3331.07, 3458.37	NH$_2$ (2')	7.5 (bs)
		CH Stretch Alkene	3080.32	CH (2, 6, 7, 6')	8.1 - 8.2 (d, d, d)
		C=O Stretch	1645.28	CH (3, 5)	8.3 (d)
		α, β unsaturated		CH (8)	7.7 (d)
		C=C Stretch	1612.49	CH (3')	6.8 (d)
		Alkene and		CH (4')	6.6 (t)
		Aromatic		CH (5')	7.3 (d)
		NO$_2$ Stretch aromatic	1340.53		
Derivative 3A (3′-Amino-4-methoxy chalcone)		NH$_2$ Stretch	3332.99, 3462.22	NH$_2$ (3')	5.2 (s)
				CH (3, 5)	7.8 (d)
		CH Stretch Alkene	3053.32	CH (7, 8)	7.6-7.7 (d, d)
		C=O Stretch	1649.14	CH (2, 6, 2')	7.3 (d, s)
		α, β unsaturated		CH (5')	7.2 (t)
		C=C Stretch	1612.49	CH (6')	7.0 (d)
		Alkene and		CH (4')	6.8 (d)
		Aromatic		OCH$_3$ (4)	3.8 (s)
		O-CH$_3$ Stretch aromatic	1093.64		

Supplementary Table 2. Results of docking studies of chalcone derivatives with standard H1N1-NA virus (PDB code: 3B7E)

| Compounds | Site-1 | | | Site-2 | | | Site-3 | | Site-4 | | 150-loop | | | | | | Others | | | | | | Total H-bonds |
	R118	R292	R371	E119	D151	E227	W178	I222	E276	E277	G147	T148	V149	K150	D151	R152	R156	R224	T242	N294	N347	Y406	
2,4-OH-2-OCH$_3$	NH...O=C	-	-	-	-	O=C-O...H-O	-	-	-	O=C-O...H-O	-	-	-	-	-	-	-	-	-	-	-	-	03
2,4-OH-3-OCH$_3$	NH...O=C	NH...O-CH$_3$	NH...O=C	-	-	O=C-O...H-O	-	-	-	O=C-O...H-O	-	-	-	-	-	-	-	-	-	-	-	OH...O-H	06
2,4-OH-4-OCH$_3$	-	NH...O-CH$_3$	NH...O=C	O=C-O...H-O	-	-	C=O...HO	-	-	-	-	-	-	-	-	-	NH...OH	-	OH...OCH$_3$	-	-	OH...O=C	07
2,4-OH-2-Cl	NH...O=C	-	-	-	-	O=C-O...H-O	-	-	-	O=C-O...H-O	-	-	-	-	-	-	-	-	-	-	-	OH...O-H	04
2,4-OH-3-Cl	NH...O=C NH...OH-C$_2$	-	-	O=C-O...H-O	-	O=C-O...H-O	-	-	-	-	-	-	-	-	-	-	-	-	-	-	-	OH...O-H OH...O=C	06
2,4-OH-4-Cl	NH...O=C	-	NH...O=C	-	-	O=C-O...H-O	-	-	-	O=C-O...H-O	-	-	-	-	-	-	-	-	-	N...Cl	-	OH...O-H	06
2,4-OH-2-NO$_2$	-	N...O=N	N...O-N	-	-	O=C-O...H-O	-	-	-	N-...HO	-	-	-	-	-	-	-	-	-	-	-	OH...O-N	04
2,4-OH-3-NO$_2$	OH...O=C	-	-	-	-	O=C-O...H-O	-	-	-	O=C-O...H-O	-	-	-	-	-	-	-	-	-	-	-	OH...O-H	05
2,4-OH-4-NO$_2$	NH...O=C	-	-	-	-	O=C-O...H-O	-	-	-	O=C-O...H-O	-	-	-	-	-	-	-	-	-	N...O-N	N...O-N N...O=N	OH...O-H	07
2,4-OH-2-OH	-	NH...OH	-	-	C=O...HO	O=C-O...H-O	-	-	C=O...HO	O=C-O...H-O	-	-	-	-	C=O...HO	-	-	-	-	-	-	-	04
2,4-OH-3-OH	-	NH...OH	-	-	-	-	-	-	C=O...HO	O=C-O...H-O	-	-	-	-	-	-	NH...OH	-	-	-	-	-	05

Compounds	Site-1			Site-2			Site-3		Site-4		150-loop						Others						Total H-bonds
	R118	R292	R371	E119	D151	E227	W178	I222	E276	E277	G147	T148	V149	K150	D151	R152	R156	R224	T242	N294	N347	Y406	
2,4-OH-4-OH	NH...O=C	-	-	-	-	O=C-O...H O	-	-	-	O=C-O...H O	-	-	-	-	-	-	-	-	-	NH...OH	-	OH...O H	05
2-NH$_2$-2-OCH$_3$	-	-	-	-	-	HNH...OH-C=O	-	-	-	HNH...OH-C=O	-	-	-	-	-	-	-	-	-	-	-	-	02
2-NH$_2$-3-OCH$_3$	-	-	-	-	-	-	-	-	-	HNH...OH-C=O	-	-	-	-	-	-	-	-	-	-	-	-	01
2-NH$_2$-4-OCH$_3$	-	-	-	HNH...OH-C=O	-	-	-	-	-	C=O, HO-C=O	-	-	-	-	-	-	-	-	H$_3$C-O...H O, H$_3$C-O...N H$_2$-C=O	-	-	-	04
2-NH$_2$-2-Cl	-	-	-	-	-	HNH...OH-C=O	-	-	-	HNH...OH-C=O	-	-	-	-	-	-	-	-	-	-	-	-	02
2-NH$_2$-3-Cl	-	Cl...N H$_2$	-	C=O...HO-C=O	-	HNH...OH-C=O	-	-	-	HNH...OH-C=O	-	-	-	-	-	-	-	Cl...N	-	-	-	-	05
2-NH$_2$-4-Cl	-	-	-	HNH...OH-C=O	-	HNH...OH-C=O	-	-	-	HNH...OH-C=O	-	-	-	-	-	-	-	-	-	Cl...N H$_2$-C=O	-	-	06
2-NH$_2$-2-NO$_2$	-	-	-	-	-	HNH...OH-C=O	-	-	-	HNH...OH-C=O	-	-	-	-	-	-	-	-	-	-	-	O=N-O...H O-Ph	03
2-NH$_2$-3-NO$_2$	-	-	-	-	-	HNH...OH-C=O	-	-	-	HNH...OH-C=O	-	-	-	-	-	-	-	O=N-O...N	-	-	-	-	03
2-NH$_2$-4-NO$_2$	ON=O...NH$_2$	-	-	HNH...OH-C=O	-	C=O, HO-C=O	-	-	-	HNH...OH-C=O	-	-	-	-	-	-	-	-	-	O=N-HNH-C=O	-	-	06

Residues

Compounds	Residues																						Total H-bonds
	Site-1			Site-2			Site-3		Site-4		150-loop						Others						
	R118	R292	R371	E119	D151	E227	W178	I222	E276	E277	G147	T148	V149	K150	D151	R152	R156	R224	T242	N294	N347	Y406	
$2\text{-}NH_2\text{-}2\text{-}OH$	-	-	-	-	-	HNH...OH-C=O	-	-	-	HNH...OH-C=O	-	-	-	-	-	-	-	-	-	-	-	OH...OH-Ph	03
$2\text{-}NH_2\text{-}3\text{-}OH$	-	-	-	-	-	HNH...OH-C=O	-	-	OH...O=C-OH	HNH...OH-C=O	-	-	-	-	-	-	-	-	-	-	-	-	03
$2\text{-}NH_2\text{-}4\text{-}OH$	-	-	-	-	-	HNH...OH-C=O	-	-	OH...O=C-OH	HNH...OH-C=O	-	-	-	-	-	-	-	-	-	-	-	-	03
$3\text{-}NH_2\text{-}2\text{-}OCH_3$	-	-	-	-	-	O=C-O...H N	-	-	-	O=C-O...H N	-	-	-	-	-	-	-	-	-	-	-	-	02
$3\text{-}NH_2\text{-}3\text{-}OCH_3$	-	-	-	-	-	CH3O...OCH3	-	-	-	CH3O...OCH3	-	-	-	-	-	-	-	-	-	-	-	-	02
$3\text{-}NH_2\text{-}4\text{-}OCH_3$	NH...O=C	-	-	-	-	O=C-O...H N	-	-	-	O=C-O...H N	-	-	-	-	-	-	-	-	-	O=C-N...OCH3	-	-	04
$3\text{-}NH_2\text{-}2\text{-}Cl$	-	-	-	O=C-O...H N	-	-	-	-	-	O=C-O...H N	-	-	-	-	-	-	-	-	-	-	-	-	02
$3\text{-}NH_2\text{-}3\text{-}Cl$	-	-	-	-	-	O=C-O...H N	-	-	-	O=C-O...H N	-	-	-	-	-	-	-	-	-	-	-	-	02
$3\text{-}NH_2\text{-}4\text{-}Cl$	-	-	-	-	-	O=C-O...H N	-	-	-	O=C-O...H N	-	-	-	-	-	-	-	-	-	-	-	-	02
$3\text{-}NH_2\text{-}2\text{-}NO_2$	NH...O=N NH...O-N	-	HN...O=N	-	-	-	-	-	-	-	-	-	-	-	-	-	-	-	-	-	-	OH...O-N	05
$3\text{-}NH_2\text{-}3\text{-}NO_2$	-	-	-	O=C-O...H N	-	-	-	-	-	-	-	-	-	-	-	-	-	-	-	-	-	-	01

Compounds	Residues																						Total H-bonds
	Site-1			Site-2			Site-3		Site-4		150-loop						Others						
	R118	R292	R371	E119	D151	E227	W178	I222	E276	E277	G147	T148	V149	K150	D151	R152	R156	R224	T242	N294	N347	Y406	
3 - NH₂-4-NO₂	-	-	-	-	-	O=C-O...H N	-	-	-	O=C-O...H N	-	-	-	-	-	-	-	-	-	-	-	-	02
3 - NH₂-2-OH	NH...O=C	-	-	-	-	-	-	-	-	O=C-O...H O	-	-	-	-	-	-	-	-	-	-	-	-	02
3 - NH₂-3-OH	-	-	-	-	C=O...HN	-	-	-	C=O...HO	-	-	-	-	-	-	NH...O=C	-	-	-	-	-	-	03
3 - NH₂-4-OH	-	-	-	-	-	O=C-O...H N	-	-	-	O=C-O...H N	-	-	-	-	-	-	-	-	-	-	-	-	02

Atoms involved in hydrogen bonding from ligand (row) to amino acid residue of H1N1-NA (column) are shown. Last column shows number of hydrogen bond observed in case of each ligand.

Supplementary Table 3. Results of docking studies of chalcone derivatives with pandemic H1N1-NA virus (PDB code: 3TI6)

| Compounds | Site-1 | | | Site-2 | | | Site-3 | | Site-4 | | | | Others | | | | | | Total H-bonds |
	R118	R292	R371	E119	D151	E227	W178	I222	E276	E277	R156	S179	N221	R224	T242	S246	N294	Y406	
2,4-OH-2-OCH₃	-	-	-	O=C-O...HO	-	O=C-O...HO	-	-	-	-	NH...OH	-	-	-	-	-	-	-	03
2,4-OH-3-OCH₃	-	-	NH...O=C	-	-	-	-	-	-	O=C-O...HO	-	OH...O=C	-	-	-	OH...OCH₃	-	OH...OH / OH...O=C	06
2,4-OH-4-OCH₃	NH...O=C	-	NH...O=C / NH...O=C	-	-	O=C-O...HO	-	-	-	O=C-O...HO	-	-	-	-	-	-	-	OH...O=C	06
2,4-OH-2-Cl	-	-	-	O=C-O...OH	-	O=C-O...OH	-	-	-	-	NH...OH	-	-	-	-	O...Cl	-	-	04
2,4-OH-3-Cl	-	-	-	-	O...HO	-	-	-	-	O=C-O...HO	-	O...O=C	-	-	-	O...Cl	N...Cl	-	05
2,4-OH-4-Cl	-	=N-...OH / =N-..HO / NH...OH	-	-	-	-	-	-	-	O=C-O...HO	NH...Cl	-	-	=N-...O=C	-	-	-	-	05
2,4-OH-2-NO₂	-	-	-	O=C-O...HO	N-C=O...HO	O=C-O...HO	-	-	-	-	NH...OH	-	-	-	-	O...O-N	-	-	04
2,4-OH-3-NO₂	-	-	-	-	-	-	-	-	-	O=C-O...HO	NH...OH	OH...O=C	-	-	-	O...O-N / O...O=N	O=C-N...O=N	-	07
2,4-OH-4-NO₂	-	=N-...OH / =N-...HO / NH...OH	-	-	-	-	-	-	O=C-O...HO	O=C-O...HO	NH...O-N / NH...O=N	-	-	N...O=C	-	-	-	-	07
2,4-OH-2-OH	-	-	-	O=C-O...HO	-	O=C-O...HO	-	-	-	O=C-O...HO	NH...OH	-	-	-	-	-	-	-	04
2,4-OH-3-OH	-	-	-	O=C-O...HO	-	O=C-O...HO	-	-	-	O=C-O...HO	NH...OH	-	-	-	-	-	CO-N...OH	-	05

Compounds	Site-1			Site-2			Site-3		Site-4		Others								Total H-bonds
	R18	R292	R371	E119	D151	E227	W178	I222	E276	E277	R156	S179	N221	R224	T242	S246	N294	Y406	
2,4-OH-4-OH	-	-N...OH NH...OH	-	O=C-O...HO	-	-	-	-	-	O=C-O...HO	NH...OH	-	-	N=...O=C	-	-	-	-	06
2-NH2-2-OCH3	-	-	-	-	-	-	-	-	-	-	-	C=O...H O	-	-	-	-	-	-	01
2-NH2-3-OCH3	-	-	-	-	-	HNH....OH-C=O	-	-	-	HNH....OH-C=O	-	-	-	-	-	-	H3C-O...NH2 -C=O	C=O...H O-Ph	04
2-NH2-4-OCH3	-	-	H3C-O....NH2	HNH....O=C-OH	-	-	-	-	-	HNH....OH-C=O	-	-	-	-	-	-	-	-	03
2-NH2-2-Cl	-	-	-	-	-	-	-	-	-	HNH....OH-C=O	-	-	-	-	-	-	-	-	02
2-NH2-3-Cl	-	Cl...N	-	-	-	HNH....OH-C=O	-	-	-	HNH....OH-C=O	-	-	-	-	-	-	-	C=O...H O-Ph	04
2-NH2-4-Cl	-	-	-	-	-	-	-	-	-	HNH....OH-C=O	Cl...NH2	-	-	Cl...N, C=O...N	-	-	-	-	04
2-NH2-2-NO2	-	-	N=O...NH2, N-O....NH2	-	-	-	-	-	-	HNH....OH-C=O	-	-	-	-	-	-	-	C=O...H O-Ph, N-O...HO-Ph	05
2-NH2-3-NO2	-	-	-	-	-	-	-	-	-	-	-	C=O...H O	-	-	-	N-O...HO	N-O...NH2 -C=O	-	03
2-NH2-4-NO2	N-O....NH2	-	N=O...NH2	-	-	HNH....OH-C=O	-	-	-	HNH....OH-C=O	-	-	-	-	-	-	-	-	04
2-NH2-2-OH	HNH....O=C-OH	-	-	-	-	-	-	-	-	HNH....OH-C=O	-	-	-	-	-	-	-	-	02

Residues

Compounds	Site-1			Site-2			Site-3		Site-4		Others								Total H-bonds
	R118	R292	R371	E119	D151	E227	W178	I222	E276	E277	R156	S179	N221	R224	T242	S246	N294	Y406	
2-NH₂-3-OH	-	-	-	-	-	HNH.... OH-C=O	-	-	-	HNH.... OH-C=O	-	-	-	-	-	HO...O H	HO...H NH	C=O...H O-Ph	05
2-NH₂-4-OH	-	-	-	OH...O H-C=O	-	-	-	-	-	-	HO....N H₂	-	-	C=O...N	-	-	-	-	03
3-NH₂-2-OCH₃	-	-	-	O=C- O...HN	-	-	C=O...H N	-	-	-	-	-	-	-	-	-	-	HO...O= C	04
3-NH₂-3-OCH₃	-	NH..O= C	NH..O= C	-	-	-	-	-	O=C- O...HN	-	NH...OC H₃	-	-	-	-	-	-	-	04
3-NH₂-4-OCH₃	-	-	-	-	-	O=C- O...HN	-	-	-	O=C- O...HN	-	-	O=C- N...OCH₃	C=N..O CH₃	-	-	-	OH...O= C	04
3-NH₂-2-Cl	-	-	-	-	-	-	C=O...H N	-	-	-	-	-	-	-	-	-	-	OH...O= C	03
3-NH₂-3-Cl	NH..O= C	-	-	-	-	-	-	-	-	-	NH...Cl	-	-	-	-	-	-	OH...O= C	03
3-NH₂-4-Cl	NH..O= C	-	-	O=C- O...HN	-	O=C- O...HN	-	-	-	O=C- O...HN	-	-	O=C- N..Cl	-	-	-	-	-	04
3-NH₂-2-NO₂	NH..O= N	-	NH..O- N	-	-	-	-	-	-	-	-	-	-	-	-	-	-	OH..O- N=O	04
3-NH₂-3-NO₂	NH..O- N	-	NH..O- N	-	-	-	-	-	-	-	-	-	-	-	-	-	-	OH..O- N	03
3-NH₂-4-NO₂	-	-	-	-	C=O..O- N	-	C=O..H N	-	C=O..H N	-	NH...O- N NH..O= N	-	-	-	-	-	-	-	04

Compounds	Residues																			Total H-bonds
	Site-1			Site-2			Site-3		Site-4		Others									
	R118	R292	R371	E119	D151	E227	W178	I222	E276	E277	R156	S179	N221	R224	T242	S246	N294	Y406	
3-NH2-2-OH	-	-	-	O=C-O...HN	-	-	-	-	-	-	-	-	-	-	-	-	-	HO...O=C	02
3-NH2-3-OH	O=C-O...HN	-	-	-	-	-	C=O...H N	-	-	-	-	-	-	-	-	O...OH	CO-N-...OH	HO...O=C	05
3-NH2-4-OH	O=C-O...HN	-	-	-	-	-	O=C-O...HN	-	O=C-O...HO	-	-	-	-	-	-	-	O=C-N...OH	HO...O=C	05

Atoms involved in hydrogen bonding from ligand (row) to amino acid residue of H1N1-NA (column) are shown. Last column shows number of hydrogen bond observed in case of each ligand.